

Behavior of the Johnson-King Turbulence Model in Axisymmetric Supersonic Flows

Yasuo Noguchi*

University of Salford, Salford, Greater Manchester M5 4WT, England, United Kingdom
and

Toshimasa Shiratori†

Tokyo Metropolitan Institute of Technology, Tokyo 191, Japan

A series of systematic tests are carried out on the Johnson-King turbulence model (JKM) for applied compressible aerodynamics. Two-dimensional flows with a moderate adverse pressure gradient and without separation at various Mach numbers are used for the tests. The results are compared with the Baldwin-Lomax model (BLM) as well as the measurements. The agreement of the results of both models and the measured data becomes poorer at higher Mach numbers. Overall, the performance of the JKM is slightly better than BLM except with respect to the prediction of the skin friction coefficient. The ordinary differential equation (ODE) in the JKM is effective in improving the prediction. However, the effects of the ODE are not as significant as in flows with separation. Use of the JKM even in nonseparated flows may improve accuracy of prediction, which has not been clearly established before this work.

Nomenclature

| | |
|--------------------|---|
| a_1 | = modeling constant, $-\overline{u'v'_m}/k_m$ |
| C_f | = local skin friction coefficient |
| C_p | = pressure coefficient |
| F_{MAX} | = maximum value of function $F(x)$ |
| k | = von Kármán constant |
| k_m | = maximum turbulence kinetic energy |
| L | = reference length |
| M | = Mach number |
| R | = radius of the body |
| Re_x | = Reynolds number based on reference length |
| t | = time |
| u, v | = velocity components in the x and y directions, respectively |
| $-\overline{u'v'}$ | = defined as Reynolds shear stress |
| x, y | = Cartesian coordinate axes |
| Y_{MAX} | = position of maximum $F(y)$ in the y direction |
| y_m | = position of $-\overline{u'v'_m}$ in the y direction |
| δ | = boundary-layer thickness |
| θ | = momentum thickness |
| μ | = viscosity coefficient |
| ρ | = density |
| $\sigma(x)$ | = nonequilibrium function in the JKM |

Subscripts

| | |
|----------|------------------------------|
| eq | = equilibrium value |
| m | = maximum value except y_m |
| w | = wall condition |
| ∞ | = freestream value |

Introduction

ONE of the most popularly used turbulence models for applied compressible aerodynamics is the Baldwin-Lomax model (BLM).¹ However, when flowfields become complex such as in an

adverse pressure gradient or with a flow separation, the model cannot accurately predict the flow because the "history effect" is not included in the model. Increasingly complex turbulence models have been employed for more complex flows in recent years. These models require significantly if not prohibitively large computing times and costs to simulate practical cases to assist design work.

Recently, Johnson and King² and Johnson³ introduced a turbulence model (JKM) that added some history effects to the simple algebraic eddy viscosity model. An ordinary differential equation (ODE) has been introduced to resolve the maximum Reynolds shear stress development in the streamwise direction to account for convection and diffusion.

Only a few reports have been published concerning the behavior of the JKM with various flow conditions. Menter⁴ compared four turbulence models including the BLM and JKM in an incompress-

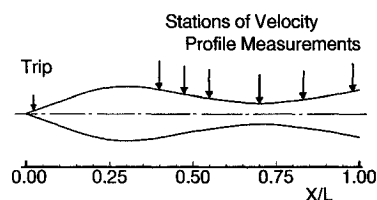


Fig. 1 Body geometry.

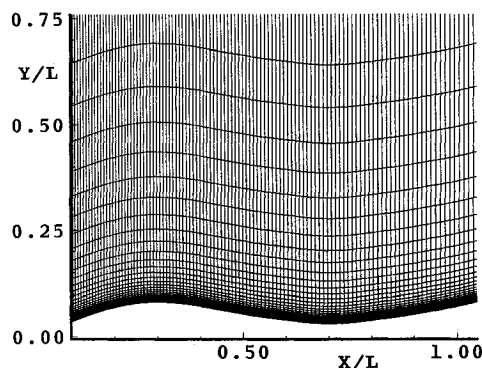


Fig. 2 Part of mesh system.

Received May 17, 1993; presented as Paper 93-3032 at the AIAA 24th Fluid Dynamics Conference, Orlando, FL, July 6-9, 1993; revision received Nov. 6, 1993; accepted for publication Nov. 11, 1993. Copyright © 1994 by the American Institute of Aeronautics and Astronautics, Inc. All rights reserved.

*Lecturer in Aerodynamics, Department of Aeronautical and Mechanical Engineering, Member AIAA.

†Associate Professor, Department of Aerospace Systems Engineering, 6-6 Asahigaoka, Hino-City, Member AIAA.

ible adverse pressure gradient flow with a separation. The JKM performed the best amongst the turbulence models compared. There are even fewer reports that systematically tested the behavior of the JKM in compressible flows. Noguchi et al.⁵ tested the JKM in a flow without a separation. He further extended the work to test the model in various Mach numbers.⁶

In this work both the BLM and JKM are compared with the measured data at four Mach numbers with a moderate pressure gradient without flow separation. Particular attention is paid to the observation of the behavior of the JKM. This is a part of the systematic testing of the JKM to clarify the behavior of the model in different flow conditions, pressure gradients, and Mach numbers.

Algorithm

The axisymmetric compressible thin-layer approximation of the Reynolds-averaged Navier-Stokes equations in conservation law form in general curvilinear coordinates are

$$\frac{\partial Q}{\partial \tau} + \frac{\partial E}{\partial \xi} + \frac{\partial F}{\partial \eta} + H = \frac{1}{Re_x} \left(\frac{\partial S}{\partial \eta} \right) \quad (1)$$

The equations are solved by the Warming-Beam⁷ explicit time-marching scheme. To damp high-frequency oscillations, fourth-order numerical dissipation terms, suggested by Warming and Beam,⁷ are added. All of the results presented here are calculated

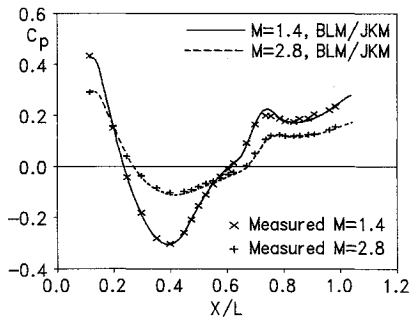


Fig. 3 Skin friction coefficient.

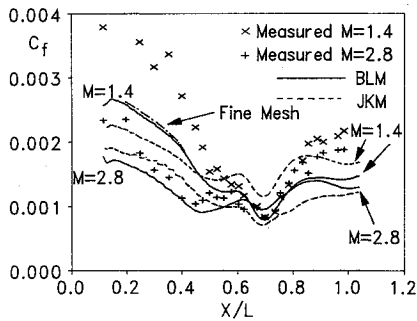


Fig. 4 Pressure coefficient.

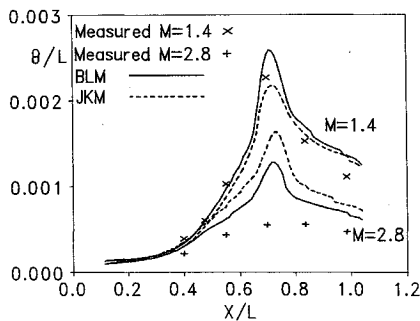


Fig. 5 Momentum thickness development.

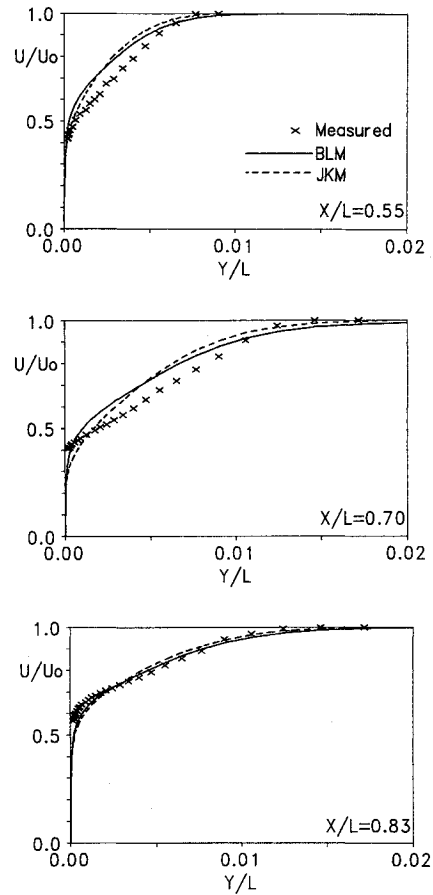


Fig. 6 Velocity profiles at $M_\infty = 1.4$.

with the far-field boundary sufficiently far away from the body to allow the freestream conditions to be used at the boundary.

Turbulence Models

The present work used the original version of the BLM,¹ which is a well-known and well-used model. The JKM^{2,3} used in this work is a slightly modified version. The function $F(y)$ used in the BLM¹ is introduced instead of using the boundary-layer thickness δ , which is rather difficult to define.

The inner region eddy viscosity is given by

$$\mu_{ti} = \rho D^2 k y (-\overline{u'v_m'})^{1/2} \quad (2)$$

The damping term $D = 1 - \exp [-(\overline{u'v_m'})^{1/2} \rho_w y / \mu_w A^+]$, where $A^+ = 15$ instead of 26 used in the BLM, and $(-\overline{u'v_m'})$ is called the Reynolds shear stress for convenience, although it should be $\rho(-\overline{u'v_m'})$. Subscript m denotes the maximum value at a given x station, and y_m indicates its distance from the wall.

The outer formulation is given by

$$\mu_{to} = \sigma(x) [\alpha C_1 \rho Y_{MAX} F_{MAX} F_{kleb}(y)] \quad (3)$$

where α and C_1 are the same as in the BLM.¹

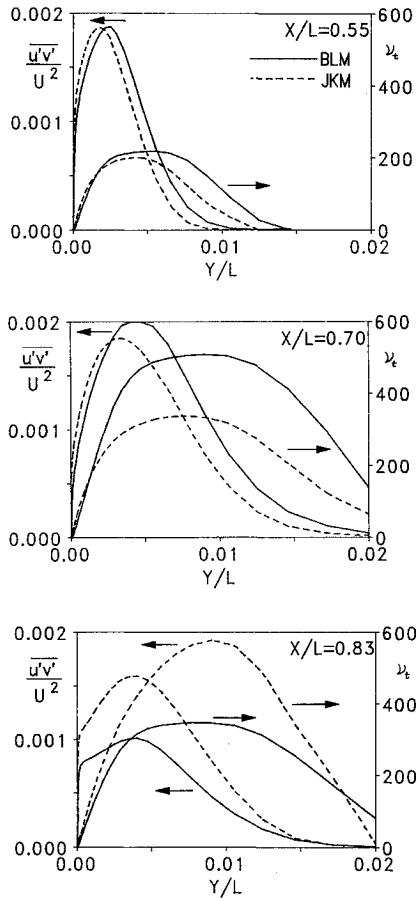
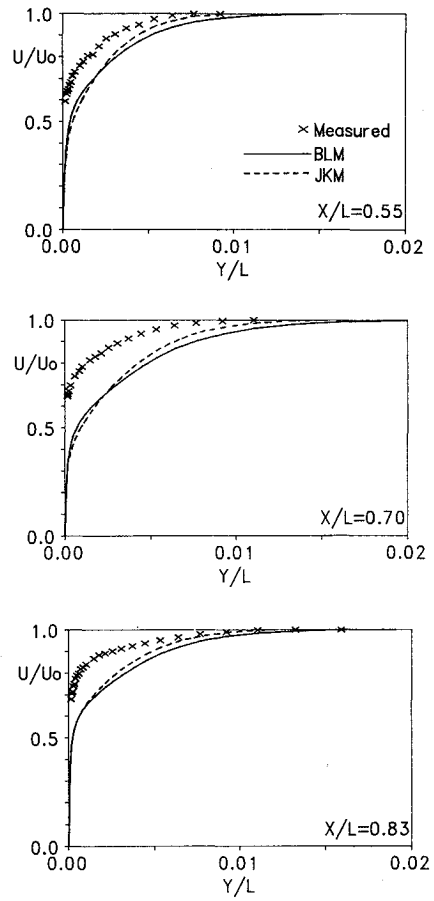
The maximum Reynolds shear stress is calculated by solving an ordinary differential equation

$$\frac{dg}{dx} = \frac{a_1}{2u_m L_m} \left\{ \left(1 - \frac{g}{g_{eq}} \right) \frac{C_{diff} L_m}{a_1 \delta [0.7 - (y/\delta)_m]} \left| 1 - \sigma(x)^{1/2} \right| \right\} \quad (4)$$

where L_m is a dissipation length scale given by

$$L_m = 0.4y_m \quad \text{for } y_m/\delta < 0.225$$

$$L_m = 0.09\delta \quad \text{for } y_m/\delta > 0.225 \quad (5)$$

Fig. 7 Shear stress and eddy viscosity profiles at $M_\infty = 1.4$.Fig. 8 Velocity profiles at $M_\infty = 2.8$.

The variables are

$$g = (-\overline{u'v'})^{-1/2} \quad (6)$$

$$g_{eq} = (-\overline{u'v'}_{meq})^{-1/2} \quad (7)$$

where eq indicates the values when the convection and diffusion are negligible or are in an equilibrium condition. The values for a_1 and C_{diff} are 0.25 and 0.5, respectively.

The equilibrium function $\sigma(x)$ is updated by two iterations ($n = 1$ and 2)

$$\begin{aligned} \mu_{tom}^{(n+1)} &= \mu_{tom}^{(n)} \frac{\tilde{\mu}_{tm}^{(n)}}{\mu_{tm}^{(n)}} \\ \mu_{tm}^{(n+1)} &= \mu_{tom}^{(n+1)} \{1 - \exp[-\mu_{tm}^{(n+1)} / \mu_{tom}^{(n+1)}]\} \\ \sigma(x)^{n+1} &= \sigma(x)^n \frac{\mu_{tom}^{(n+1)}}{\mu_{tom}^{(n)}} \end{aligned} \quad (8)$$

where $\tilde{\mu}_{tm}$ is the maximum eddy viscosity calculated by Eq. (4).

Body Geometry and Mesh

The turbulence models are applied to a waisted body of revolution, for which Winter et al.⁸ made a series of detailed measurements at various Mach numbers. The geometry of the waisted body is shown in Fig. 1. The cases chosen for the present comparisons are the freestream Mach numbers at $M_\infty = 1.4, 2.0, 2.4$, and 2.8 with the length based Reynolds numbers of nominally $Re_x = 1.0 \times 10^7$.

At first only the conical nose part up to $X/L = 0.11$ is calculated using the BLM. The turbulence model is switched on at the same location as the transition trip in the experiments ($X/L = 0.025$). The grid used for this part has 65 points each in the X and Y directions. The results at $X/L = 0.1$ are then used as the starting conditions to calculate the downstream part of the body.

The coordinate system used for the afterbody calculations has 115 and 65 points in the X and Y directions, respectively, as seen in Fig. 2. The results were compared with the results from the 124×80 mesh. Both results are almost identical as shown in Fig. 3, and this suggests that the results are nearly mesh independent. The values of Y^+ at the first grid points are between 0.13 and 0.5 at the stations compared with the experiment.

Results and Discussion

The pressure coefficient developments predicted by both models are almost identical and agree very well with the measured data. The agreements are good at all of the Mach numbers tested. Figure 4 shows the pressure coefficient developments at $M_\infty = 1.4$ and 2.8.

However, the skin friction prediction shows poor agreement with the measurements as shown in Fig. 3. Although both models do not agree with the measured data, the BLM results are better, especially with respect to the prediction of the lowest levels of skin friction coefficient, than the JKM. The skin friction drag discrepancies from the measured data are approximately 30% for both the BLM and JKM at $M_\infty = 1.4$ and 6 and 10% at $M_\infty = 2.8$ for the BLM and JKM, respectively.

Figure 5 shows the development of momentum thickness. At $M_\infty = 1.4$ the results from both models agree well with the measured data except the peak value at $X/L = 0.7$. However, the agreement with the measured data at $M_\infty = 2.8$ is poor for both models. Generally, the JKM shows slightly better trends.

The velocity profiles at $M_\infty = 1.4$ at $X/L = 0.55, 0.7$, and 0.833 are shown in Fig. 6. Figure 7 shows corresponding shear stress and eddy viscosity profiles. The velocity profiles do not agree very well at $X/L = 0.55$ and 0.7 , which are in the adverse pressure gradient region. The velocity profiles agree better at $X/L = 0.833$, which is in the favorable pressure gradient region. The differences in the shear stress and eddy viscosity profiles between the two models are large at $X/L = 0.7$ and 0.833 , although these are associated with only small variations in the velocity profiles.

Figures 8 and 9 show the velocity profiles and shear stress and eddy viscosity profiles at $M_\infty = 2.8$, respectively. It is clearly shown that the boundary-layer thickness was overpredicted by both of the models and reflected in the momentum thickness development in Fig. 5. The variations between the two models in the shear stress and eddy viscosity profiles are similar to those at $M_\infty = 1.4$.

The peaks of all of the shear stress profiles produced by the JKM are closer to the wall, and this trend seems to be producing a closer agreement with the measurements than the BLM in the log law region as reported by Noguchi.⁶ Neither model produced clearly better velocity profiles agreement with the measured ones at the outer part.

The development of maximum shear stress at $M_\infty = 1.4$ and 2.8 is shown in Fig. 10. The delay in the development of the maximum shear stress by the JKM produced larger and fuller shear stress profiles at $X/L = 0.7$ by the BLM. The delays in the development produced by the JKM become clearer at higher Mach numbers. Although the differences between the two models are clear and large, it did not produce very different results in boundary-layer parameters such as momentum thickness developments.

The variation in the development of the nonequilibrium function $\sigma(x)$, which is defined in Eq. (8), increases with increase in Mach

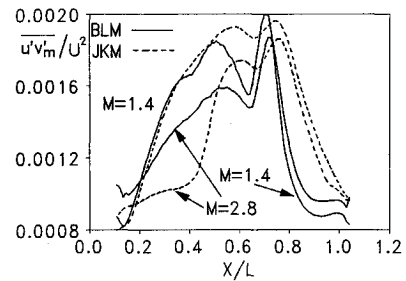


Fig. 10 Maximum shear stress development.

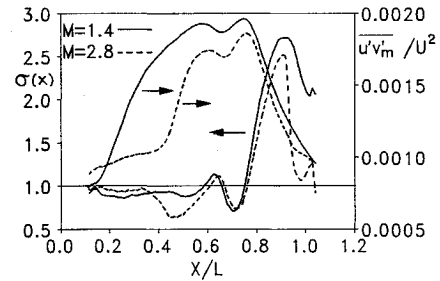


Fig. 11 Nonequilibrium function development.

number as shown in Fig. 11. The BLM is based on the assumption of an equilibrium state, i.e., the turbulence production term is equal to the dissipation term. The development of the nonequilibrium function clearly shows the nonequilibrium nature of the flow. However, the large variations in $\sigma(x)$ did not produce the significant improvements over the BLM results that were seen in separated flow cases. In separated flows a small variation in $\sigma(x)$ produced relatively small improvements in boundary-layer parameters. These small improvements produced a small movement in the position of separation. This small shift in the separation position, however, may lead to a significantly more accurate overall prediction. Nonseparated flows do not have a significant factor such as separation position that can dominate the overall accuracy of prediction.

Winter et al.⁸ carried out calculations based on the integration of the momentum and kinetic energy boundary-layer equations. The axisymmetry was introduced with the factor $1 + (y/R)$ in the integrals of boundary-layer parameters. The results show good agreement with the measured data at $M_\infty = 1.4$. They reported that the inclusion of axisymmetry may be important for the momentum thickness development prediction. Since the two models used here do not include axisymmetry, the discrepancies between the predictions and measurements may partly be caused by the streamline convergence of the actual flowfield.

Concluding Remarks

A series of tests are carried out on the BLM and JKM with moderate pressure gradient without separation at various Mach numbers.

The agreement of the results of both models and the measured data become poorer at higher Mach numbers. Overall, the performance of the JKM is slightly better than the BLM except with the prediction of skin friction. The ordinary differential equation in the JKM is effective in improving the prediction in general. However, the effects are not as significant as in flows with separation.

Use of the JKM even in nonseparated flows may improve the accuracy of prediction, and this has not been clearly established before this work. More work on the JKM at the border of separated and nonseparated flows should be carried out to observe the behavior of the model, especially the effect of the ODE.

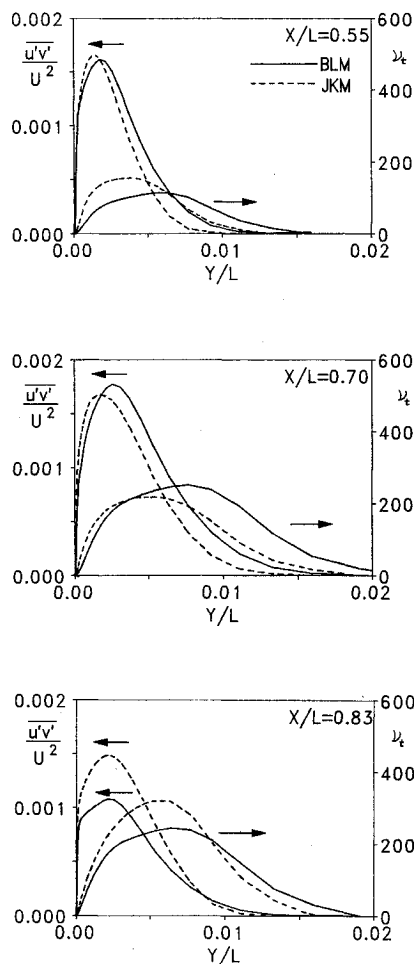


Fig. 9 Shear stress and eddy viscosity profiles at $M_\infty = 2.8$.

Acknowledgment

The authors gratefully acknowledge the British Council in Tokyo for offering a travel grant to this Anglo/Japanese collaborative research project.

References

- ¹Baldwin, B. S., and Lomax, H., "Thin Layer Approximation and Algebraic Model for Separated Turbulent Flows," AIAA Paper 78-0257, 1978.
- ²Johnson, D. A., and King, L. S., "A Mathematically Simple Turbulence Closure Model for Attached and Separated Turbulent Boundary Layers," *AIAA Journal*, Vol. 23, No. 11, 1985, pp. 1684-1692.
- ³Johnson, D. A., "Transonic Separated Flow Predictions with an Eddy-Viscosity/Reynolds Stress Closure Model," *AIAA Journal*, Vol. 25, No. 2, 1987, pp. 252-259.
- ⁴Menter, F. R., "Performance of Popular Turbulence Models for At-

tached and Separated Adverse Pressure Gradient Flows," *AIAA Journal*, Vol. 30, No. 8, 1992, pp. 2066-2072.

⁵Noguchi, Y., Hillier, R., and Graham, J. M. R., "Computation of Viscous Supersonic Flows," *Proceedings of the AGARD Symposium on Missile Aerodynamics* (Friedrichshafen, Germany), AGARD CP 493, April 1990.

⁶Noguchi, Y., "Comparison of Computational and Experimental Results in Axi-Symmetric Supersonic Turbulent Flows," *Computational Methods and Experimental Measurements VI, Vol. 1: Heat and Fluid Flow*, Computational Mechanics Publications, Southampton, England, UK, 1993, pp. 353-368.

⁷Warming, R. F., and Beam, R. M., "Upwind Second Order Difference Scheme and Applications in Aerodynamic Flows," *AIAA Journal*, Vol. 14, No. 9, 1976, pp. 1241-1249.

⁸Winter, K. G., Rotta, J. C., and Smith, K. G., "Studies of the Turbulent Boundary Layer on a Waisted Body of Revolution in Subsonic and Supersonic Flow," Royal Aircraft Establishment, Bedford, England, UK, RAE R&M 3633, 1968.



To order

Order reference:

WP/DISK-1 (WordPerfect/DOS)

MW/DISK-2 (Microsoft Word/Macintosh)

by phone, call 800/682-2422, or

by FAX, 301/843-0159

For mail orders:

American Institute of
Aeronautics and Astronautics
Publications Customer Service
9 Jay Gould Court, PO Box 753
Waldorf, MD 20604

\$50.00 per copy

Postage and handling charges:

1-4 items \$4.75 (\$25.00 overseas)

5-15 items \$12.00 (\$42.00 overseas)

All orders must be prepaid. Checks payable to AIAA, purchase orders (minimum \$100), or credit cards (VISA, MasterCard, American Express, Diners Club)

Add 5500+ new technical aerospace terms to your WordPerfect® or Microsoft Word® spell-checkers

Based on terminology in AIAA's Aerospace Database, **AeroSpell™** integrates easily into your existing spell checker, automatically helps produce more accurate documents, and saves you valuable search time.

The word list includes aerospace, chemical, and engineering terminology, common scientific and technical abbreviations, proper names, and much more.

Package includes 5.25" and 3.5" HD diskettes and installation instructions for **WordPerfect®** and **WordPerfect® for Windows** (DOS) or **Microsoft Word®** (Macintosh).



American Institute of
Aeronautics and Astronautics